"Innate transcriptional effects by adjuvants on the magnitude, quality and durability of HIV Envelope responses in NHP"

Supplementary Material

Supplementary Methods

ANE formulation.

ANE (Adjuvant Nanoemulsion) has a very similar composition to MF59, which has been previously described[1]. In brief, ANE is a Squalene-in-water emulsion comprised of 4.3% Squalene, 0.5% Span 85, 0.5% Tween 80 (w/w), that can be modified using excipients to co-deliver antigen and TLR agonists like small molecule immune potentiators (SMIP).

Animal sampling.

For NHP, peripheral blood was sampled from the femoral artery. Mucosal sampling was performed from the rectal mucosa using dry transport swabs (Fisher Scientific). Lymph node biopsies were taken from the axillary or inguinal lymph node groups. For mice, serum sampling was performed from the tail vein. Blood was collected into a microtainer serum separator tube (VWR) and centrifuged 10-20 minutes at 7000 rpm to separate serum from the clot.

Flow cytometry antibodies.

For stimulation: CD28 Ax 680 (clone CD28.2), CD49d (BD Pharm.). For surface staining: CD4 PE Cy5.5 (clone S3.5), CD8 QD655 (clone RPA-T8), CD95 APC (BD Pharm.), CD45RA TRPE (Beckman), and CCR7 Pacific Blue (BioLegend). For ICS: IFNγ FITC, TNFα PE Cy7, IL-2 PE, and CD3 APC Cy7 (all BD Pharm.)

Antibody titer half-life analysis.

Nonlinear mixed models were used for assessment of antibody titer half-life in the decay period following the week 24 immunization (Figure S8). Conditional on random effects for β_0 and β_1, we fit an exponential decay model:
$y = (\beta_1 - \beta_0)e^{-\beta 2t} + \beta_0 + \varepsilon$

to titer data at- and post- peak collected in the week 26-89 range, separately for each study group, where y is the observed antibody titer, t is the number of weeks elapsed since the peak titer measurement, β_1 is the mean peak titer at time $t = 0$, β_0 is the mean titer set-point, β_2 is the mean exponential rate of decay, and ε is a normally distributed error. Fixed effects were estimated using the maximum likelihood method implemented in *R*'s nlme function. An animal's titer half-life was estimated as:
$\log \{(\hat{\beta}_1 - \hat{\beta}_0)/(\hat{\beta}_1/2 - \hat{\beta}_0)\} / \hat{\beta}_2$ *weeks.*

Whole blood RNA collection and extraction.

2.5mL of peripheral whole blood was sampled from the femoral artery and collected into PAXgene blood RNA tubes (PreAnalytiX, Qiagen) per the manufacturer's instructions. RNA was extracted according to manufacturer instructions using the manual method. Yield and quality of extracted RNA was confirmed using the RNA6000 Chip on a 2100 Bioanalyzer (Agilent). RNA samples were collected prior to

vaccination and 4, 24, and 72hrs and 14 days post-vaccination. The complete RNA sample table is provided in Table S2. We note that technical replicate arrays were run for one RNA sample for the 24hr time point of the polyIC:LC group NHP A4E002:
20101214_WholeB_VivoIM_EnvC_PolyICLC_024hr_A4E002_AgilentRmE_BotL.txt
20110208_WholeB_VivoIM_EnvC_PolyICLC_024hr_A4E002_AgilentRmM_BotR.txt.

HIV-1 neutralization assay.

Neutralization was measured using single-round-of-infection HIV-1 Env-pseudoviruses and TZM-bl target cells, as described previously [2-4]. Neutralization curves were fit by nonlinear regression using a 5-parameter hill slope equation as previously described [3]. 50% inhibitory concentrations (ID_{50}) are reported as the reciprocal serum dilution required to inhibit infection by 50%.

HIV-1 specific binding antibody assays.

Plasma HIV-1 specific antibodies to HIV-1 gp140 proteins were measured by a custom HIV-1 binding antibody multiplex assay as previously described [5-7]. Plasma IgG antibody titers (area under the curve, AUC) were determined by serial dilutions of rhesus plasma (1:80, 7-fold). Plasma IgA antibody responses were measured at a 1/40 dilution. Rectal IgG was measured from elutions from rectal wicks. Mucosal MFI values normalized to total IgG concentrations (Specific Activity MFI*dil/μg/ml IgG). The following antigen was provided by Drs. Liao/Haynes, Duke University: Subtype C Envelope (6): o-gpTV1deltaV2. All assays were run under GCLP compliant conditions, including tracking of positive controls by Levy-Jennings charts using 21CFR Part 11 compliant software. Positive controls included a HIVIG, CH58 mAb, and CH31 mAb IgG titration. Negative controls included in every assay were blank beads, HIV-1 negative sera, and baseline (pre-vaccination) samples. To control for antigen performance, we used the preset criteria that the positive control titer (HIVIG) included on each assay had to be within +/- 3 standard deviations of the mean for each antigen (tracked with a Levy-Jennings plot with preset acceptance of titer (calculated with a four-parameter logistic equation, SigmaPlot, Systat Software). Antibody measurements were acquired on a Bio-Plex instrument (Bio-Rad, Hercules, CA) using 21CFR Part 11 compliant software and the readout is in MFI. The preset assay criteria for sample reporting were: coefficient of variation (CV) per duplicate values for each sample were ≤15% and >100 beads counted per sample.

Avidity assay.

The gp120 C1 mAb A32 and the V3 mAb 19b were supplied by James Robinson (Tulane University, LA). The following antigen was used in the SPR experiments: TV1 gp140. Vaccinee IgG avidity measurements were done by surface plasmon resonance analysis as described previously [8-10]. SPR experiments were run on a BIAcore 4000 instrument (BIAcore/GE Healthcare) using the multiplex array format (1x16) in which each IgG samples were flowed over duplicate spots of 8 different Env antigen surfaces. Using a Series S CM5 chip (BIAcore/GE Healthcare) proteins were amine coupled in duplicate on 16 different spots on four flow channels of the chip. The negative control mAb Synagis (anti-RSV) was flowed over each surface and the signal was used to subtract out non-specific interactions with each individual spot. Each of the Env proteins were immobilized to about 5000-15000 RU, and the V3 peptide to about 400-600 RU using amine coupling chemistry as described earlier [8]. Antigen surface activity was monitored using the C1 mAb A32 or 19b as positive controls and Synagis mAb as negative control. The IgG samples were diluted in PBS to 200ug/mL and injected over each of the flow cells with replicate spots (2x) at 30uL/min for an association time of 150 s and a dissociation time of 600s. Following each binding cycles, surfaces were regenerated with two short injection (20s) of glycine, pH2.5. Each surface activity was monitored by including A32 (20ug/mL) or 19b (5ug/mL) injection at regular interval of every 20 cycles of samples and surface decay of control mAb binding over the entire experimental run was used to normalize binding signal of plasma IgG samples. Decay in surface activity was corrected by normalization of IgG binding responses to control mAb binding in the BIAcore 4000 Methods program. Data analyses

were performed with BIAevaluation 4000 and BIAevaluation 4.1 software (BIAcore/GE Healthcare) as described earlier [8,10]. Kinetic binding responses were measured by averaging post-injection response unit (RU) over a 10s window and dissociation rate constant, kd (s-1) was measured during the post-injection/buffer wash phase (after the first 10s to allow stabilization of signal) following curve fitting to a Langmuir dissociation equation. A relative avidity binding score was calculated for each IgG sample as follows, Avidity score (RUs) = Binding Response (RU)/kd, s-1, with higher binding responses and slower Kd as an indicator of higher affinity interaction.

Microarray annotation

A multi-tiered approach was employed to annotate the Agilent rhesus macaque microarray probes to enable subsequent module-based and enrichment analysis. First, the microarray probes that align to human exon sequences were identified and annotated according to the associated human gene identifiers. Microarray probes that do not align to human exons were aligned to macaque exon sequences or macaque transcript sequences. These were annotated with the corresponding macaque gene identifiers, which were then mapped to human gene identifiers using Homologene (https://www.ncbi.nlm.nih.gov/homologene). Probes that did not align to either human or macaque sequences were annotated by Homologene mapping from the original Agilent annotations to human. Analyses were performed at the level of gene symbols (human when possible, otherwise macaque).

Microarray normalization

Microarrays were quantile normalized using the *normalize.quantiles* function in the *preprocessCore* Bioconductor package [11]. Following our previous studies [12], repeated gene expression measurements for aligned genes were collapsed in the following manner prior to analysis: (i) first, simple log2 averages were computed for repeated measurements of individual probes; and then (ii) weighted log2 averages based on 90% expression quantiles were computed for distinct probes that aligned to the same gene. This generated a 27346 gene X 225 sample gene expression matrix.

Gene pre-filtering

Prior to analysis, genes with very low expression were excluded. This was accomplished by filtering out genes with 90% expression quantiles (computed over all time points and NHPs) that did not exceed a normalized log2 expression value of 6, leaving a 19205 by 225 (gene by sample) expression matrix. The (gene by sample) normalized expression matrix was then transformed into a matrix of gene expression log2 fold-changes by comparing expression values in each animal at each post-vaccination time point (4, 24, 72, and 336hrs) to pre-vaccination expression values in the same NHPs. This matrix was arranged so that log2 fold-changes for each gene at each time point were in rows and each NHP was represented in a single column. The resulting matrix consisted of 76820 rows (genes X time points) and 53 columns (NHPs). (Gene X time point) combinations with log2 fold-changes that did not differ appreciably between NHPs and did not exhibit gross responsiveness compared to pre-vaccination were excluded. This was accomplished by filtering out gene x time point combinations with log2 fold-change standard deviations ≤ 0.5 (computed across all NHPs) and filtering out gene x time point combinations for which 10 or fewer NHPs exhibited absolute log2 fold-changes > 0.5. The resulting matrix consisted of 36311 rows (genes X time points) and 53 columns (NHPs) (Supplementary Table 1_MatrixOfFilteredLog2FoldChanges). Of the two technical replicates for the 24 hour sample of the pIC:LC group NHP A4E002, only one was used for computing the fold-changes (20101214_WholeB_VivoIM_EnvC_PolyICLC_024hr_A4E002_AgilentRmE_BotL.txt). The other replicate (20110208_WholeB_VivoIM_EnvC_PolyICLC_024hr_A4E002_AgilentRmM_BotR.txt) was not used in the analyses.

Module-based expression analysis

Prior to performing statistical analysis of the gene expression patterns, a module-based (meta-gene X time point) log2 fold-change matrix was constructed from the (gene X time point) log2 fold-change matrix using pre-defined gene sets of functionally associated co-expressed genes. This (meta-gene X time point) log2 fold-change matrix facilitates functional interpretation of gene expression data and complements the analysis based on individual genes.

Three gene sets were used to construct the module-based fold-change matrix. 1) the annotated subset of "*Chaussabel modules"*, described in [13] and downloaded from (http://www.biir.net/public_wikis/module_annotation/G2_Trial_8_Modules); 2) *Blood transcriptional modules (BTMs)*, described in [14]; and 3) *injection-site* modules we derived from adjuvant-induced transcriptional responses measured previously in mouse muscle [15].

We derived transcriptional modules from the murine adjuvant study in the following manner: First, the matrix of gene expression fold-changes (SD1.xls) of the 1200 adjuvant-responsive genes in mouse muscle at 6 time points post-injection (3, 6, 12, 24, 48, 96hrs) was downloaded from [15]. Gene expression fold-changes for genes represented by multiple probes in the matrix were averaged. For each gene, the fold change at the time point with the maximum observed absolute log2 fold-change was taken as representative and then discretized (-1 if ≤ 1; 1 if ≥ 1; 0 otherwise), giving a single discretized value for each gene for each adjuvant. Finally, genes were grouped according patterns of discretized regulation observed across the 5 adjuvant conditions (PBS, MF59, CpG, MF59+CpG, and alum) and patterns with 10 or more member genes were retained as modules. Mouse gene IDs were mapped to human using Ensembl. Prior to computing module-based expression fold-changes, an updated homology table was obtained from Homologene (https://www.ncbi.nlm.nih.gov/homologene; April 29th, 2016 build) and used annotate several macaque-specific genes that had not been assigned human orthologs during the initial annotation.

The (meta-gene X time point) log2 fold-change matrix was derived from the (gene X time point) log2 fold-change matrix and gene sets using the following procedure, which was applied to each individual gene set at each time point. First, the genes from the selected gene set that survived the pre-filtering at the chosen time point were identified. The 25% trimmed mean of the log2 expression fold-changes of the selected genes was then computed. Pearson and Spearman rank correlations between the trimmed mean and the expression fold-changes of the individual selected genes were then computed. Genes for which both correlation coefficients were ≥ 0.5 were deemed "coherent" and retained. If 10 or more genes for the selected gene set at the chosen time point were coherent, the final meta-gene vector of log2 fold-changes for the gene set was computed by averaging over the log2 fold-changes of the coherent genes.

After the module-based log2 expression fold-change matrix was computed for all 53 NHPs, we performed an outlier analysis to determine whether the module-based expression profile for any particular animal was discordant compared to the others. Given the large amount of missing data at the 14 day time point, this analysis was performed using only the other time points, with sporadic missing data being imputed using the *Multivariate Imputations by Chained Equations* (*mice*) package in R with *predictive mean matching*. Density-based local outlier factor scores were then computed for each NHP using the lofactor function in the *Data Mining with R* (*DMwR*) package. The analysis identified NHP A4E002 from the pIC:LC adjuvant group as a strong outlier (lofactor score = 4.0, compared to a max lofactor score of 1.4 for all other animals). For this reason, NHP A4E002 was excluded from the transcriptional analyses involving either gene-level or module-based meta-gene expression.

Repeating the procedure for constructing the (meta-gene X time point) log2 fold-change matrix with the outlier NHP A4E002 excluded yielded a final 225 by 52 (meta-gene X time points by NHPs) matrix (Supplemental Table 6). The genes that were used to compute the module-based log2 expression fold-changes at each time point are provided in (Supplemental Table 5).

Univariate analysis to identify adjuvant-specific gene and meta-gene expression responses

The superset of genes and meta-genes exhibiting expression patterns that differed significantly between adjuvants at specific time points was identified using the heteroskedastic one-way test (*oneway.test* from the *stats* package in R) at a Benjamini-Hochberg FDR-adjusted p-value threshold of 0.01. Genes that survived the FDR cutoff were additionally filtered for significance at a nominal p-value threshold of 0.005.

From within the responsive superset, genes and meta-genes with expression at specific time points that were significantly up- or down-regulated compared to the no adjuvant NHP group were identified. This was performed by comparing 95% confidence intervals computed from pair-wise heteroskedastic t-tests involving the no adjuvant group and the specific adjuvant group of interest. In this manner, the complete set of significantly differentially expressed genes and meta-genes for each adjuvant group were identified (Supplemental Tables 4, 8 – lists of significant genes and meta-genes for each adjuvant group). Significant associations between gene or meta-gene groups up- or down-regulated by each adjuvant were identified by pair-wise Fisher Exact Tests comparing all gene groups (Supplemental Tables 9-10).

Patterns of adjuvant-regulated expression were further refined by determining which of the adjuvant responsive genes and meta-genes differed significantly compared to the NHP group that received alum alone. As in the case of the no adjuvant group comparisons, this was done by computing 95% confidence intervals from pair-wise heteroskedastic t-tests. In this manner, alum-induced responses were used as a frame of reference to which the responses induced by other adjuvants were compared.

Taking alum as a reference adjuvant, the superset of up-regulated genes and metagenes was then defined as those that were either significantly up-regulated in the alum alone group compared to the no adjuvant group or were significantly up-regulated in the other adjuvant groups compared to both the no-adjuvant group and the alum alone group. Similarly, the superset of down-regulated genes and metagenes was defined as those that were either significantly down-regulated in the alum alone group compared to no adjuvant group or were significantly down-regulated in the other adjuvant groups.

For the up- and down-regulated gene groups, adjuvant-specific gene regulatory patterns were then defined by assigning codes to genes and meta-genes at specific time points according to how the expression levels for a given adjuvant compared to the no vaccine group or the group that received alum by itself. For up-regulated genes & meta-genes, an adjuvant was coded as “+1” if it was significantly up-regulated compared to the no-adjuvant group, “+2” if it was significantly up-regulated compared to the no-adjuvant group and the alum only group, “-1” if it was significantly down-regulated compared to the alum only group, “-2” if it was significantly down-regulated compared to the alum only group and the no-adjuvant group, and “0” otherwise. For down-regulated genes/meta-genes, an adjuvant was coded as “-1” if it was significantly down-regulated compared to the no-adjuvant group, “-2” if it was significantly down-regulated compared to the no-adjuvant group and the alum only group, “+1” if was significantly down-regulated compared to the alum only group, “+2” if was significantly up-regulated compared to the Alum only group and the no-adjuvant group, and “0” otherwise. All up-regulated and down-regulated genes were coded in this manner and then clustered using hierarchical clustering within the *heatmap.2* function in R ({gplots}).

Systems serology methods

Isolation of HIV Env-specific IgG

IgG samples were passed over individual biotinylated recombinant TV1 gp120 protein embedded columns. The bound antibody was eluted from the column in 0.1 M citric acid, pH 2.9. The purified IgGs were treated with PNGase enzyme (NEB) to release N-linked glycans [16]. Proteins were precipitated in ice-cold ethanol and the glycan containing supernatants were dried via CentriVap. Dried glycans were fluorescently labeled with a 1:1 ratio of 50mM APTS (8-aminoinopyrene-1,3,6-trisulfonic acid, Life Technologies) in 1.2M citric acid and 1M Sodium cyanoborohydride in tetrahydrofuran (Sigma-Aldrich) at 55°C for 2 hrs. Labeled glycans were dissolved in ultrapure water (Invitrogen) and excess unbound APTS

was removed using Bio-Gel P-2 (Bio-rad) size exclusion columns. Samples were run with a LIZ 600 DNA ladder in Hi-Di formamide (Life Technologies) on an ABI 3130Xl DNA sequencer. Data was analyzed using GeneMapper software and peaks were assigned based on migration of known standards and glycan digests. Peak area was calculated. Relative percentage of each glycan structure is reported and compared.

THP1 phagocytosis (ADCP) assay

The THP1 phagocytosis assay of antigen coated beads was conducted as previously described [17]. Briefly, recombinant TV1 gp120 proteins were biotinylated with Sulfo-NHS-LC Biotin (Pierce). The proteins were then incubated with 1 μm fluorescent neutravidin beads (Invitrogen) at 4°C for 16 hrs. Excess antigen was washed away. Antigen coated beads were incubated with IgG samples (100ug/ml) 1 hr at 37°C. 1x10^5 THP1 cells were added per well and incubated at 37°C for 16 hrs. Bead uptake was measured in fixed cells using flow cytometry on a BD LSRII equipped with high-throughput sampler. Phagocytic scores are presented as the integrated MFI (%frequency × MFI/10,000) [18] (Supplementary Methods). ADCP experiments for individual IgG samples were performed in duplicate in two independent experiments.

ADCC assay

A modified rapid fluorometric ADCC (RFADCC) assay was used [19,20]. CEM-NKr CCR5+ T lymphoblast cell line (NIH AIDS reagents) was pulsed with recombinant TV1 gp120 protein (60 µg/ml) for 1 hr at RT and labeled with intracellular dye CFSE (Sigma) and membrane dye PKH26 (Invitrogen). NK cells were isolated from healthy donor whole blood with RosetteSep (Stem Cell Technologies). Purified IgG (100ug/ml) was added to the labeled CEM-NKr cells ($2x10^4$ per well), incubated with NK cells (2x105 cells per well) for 4 hr at 37°C and fixed. The proportion of PKH26+ cells lacking intracellular CFSE staining (i.e. percent (%) dead cells) was determined using flow cytometry (Supplementary Methods). RFADCC experiments for individual IgG samples were tested in two independent experiments.

Ab-dependent NK cell activation

Briefly, ELISA plates (Thermo Fisher NUNC MaxiSorp flat bottom) were coated with recombinant TV1 gp120 proteins (300ng/well) or BSA as a negative control at 4°C for 16hrs. 25ug of purified IgG were added to each well. NK cells were isolated from whole blood from healthy donors with RosetteSep (Stem Cell Technologies). $5x10^4$ NK cells, α–CD107α–phycoerythrin (PE)–Cy5 (BD), brefeldin A (10 mg/ml) (Sigma) and GolgiStop (BD) were added to each well for 5 hrs at 37°C. Cells were stained for surface markers α–CD16–allophycocyanin (APC)–Cy7 (BD), α–CD56-PE-Cy7 (BD) and α–CD3–AlexaFluor 700 (BD), then stained intracellularly with α–IFNγ–APC (BD) and α– MIP1β–PE (BD) using Fix and Perm A and B solutions (Invitrogen). Fixed cells were analyzed by flow cytometry. NK cells were defined as CD3- and CD16/56+. Ab-dependent NK cell activation assays were performed in duplicate with two independent donor NK cells.

Antibody-dependent complement deposition (ADCD) assay

The ADCD assay was adapted from the modified RFADCC assay where the CEM-NKr CCR5+ T lymphoblast cell line (NIH AIDS reagents) was pulsed with recombinant TV1 gp120 protein (60 µg/ml) or left unpulsed for 1 hr at RT and then washed to remove excess antigen. Both pulsed and unpulsed cells were then mixed with IgG samples (100ug/ml) for 15mins, followed by the addition of fresh plasma diluted in veronal buffer (1:10) and 0.1% gelatin for 20mins at 37°C. Cells were then washed and stained with CD3b-FITC (Cedarlane). The proportion of CD3b+ cells in pulsed to unpulsed conditions were determined using flow cytometry. ADCD experiments for individual IgG samples were tested in duplicate with two independent complement donors.

Associations between innate (gene expression) and adaptive immune responses

The functional significance of the adjuvant-induced gene and meta-gene expression responses was investigated by integrating them with the adjuvant-induced adaptive immune responses (Ab binding titers, IFNγ and IL4 ELISpot, and systems serology). We considered the innate (gene and meta-gene) and adaptive immune responses to be linked if they shared the same pattern of regulation across the adjuvant groups and were significantly correlated when evaluated animal-by-animal. In contrast to the gene and meta-gene expression responses, which were profiled at multiple time points and analyzed as fold-changes, the adaptive immune responses were analyzed at a single time point (14 weeks-post primary vaccination). Prior to analysis, the adaptive immune response and systems serology datasets were pre-filtered, reduced, and transformed as described below.

Pre-processing of the adaptive immune response datasets to facilitate integrations

Anti-Env IgG titers (Fig. 1A) were log10 transformed before performing univariate analysis. Prior to analysis of the IFNγ and IL-4 ELISpot datasets (Fig. 1D), values were subjected to the transformation: *transformed ELISPOT = log10(ELISPOT+1)*

Within the systems serology dataset, readouts that contained less than 20 unique values within the set of 52 NHPs (after excluding the pIC:LC outlier, A4E002) were excluded. This resulted in elimination of *IndividualG0FB*, *Antigen-specific Individual G0FB*, and *Antigen-specific Individual G1* parameters. Of the remaining parameters, the following were approximately linear in scale and were not transformed prior to analysis: NK responses (CD107a, IFNγ, MIP1β), functional responses (ADCD, ADCC, ADCP), glycosylation (total, individual, antigen-specific, with/without sialylation G0, G0F, G0B, G1, G1F, G1F.1, G1B, G1S1, G1S1F, G2 G1FB, G2F, G2B, G2FB, G2S1, G2S1F, G2S1B, G2S2, G2S2F, G2S2B, G2S2FB, fucose, bisecting, di sialic acid, mono sialic acid, and total sialic acid).

These remaining assays included measurement of eleven Fc-receptor and other specificities (Rh.R3A.3, Rh.R3A.1, Rh.R2B.1, Rh.R2A.4, Rh.R2A.3, Rh.R2A.2, huFcgRIIIb, huFcgRIIIa.V158, huFcgRIIa.R131, huC1q, and aRhIgG.PE) for 26 antigens (1086gp120, 504832 peptide, Barouch Clade C gp140 trimer, HIV1 p7, NL4 3 Integrase, RSC3, RhFLSC, SOSIP, gp120 96ZM651, gp120 Bal, gp120 CM235, gp120 Du151, gp120 JRCSF, gp120 TRO, gp120 TV 1, gp120 YU2, gp120 ZM109F, gp140 BR29, gp140 SF162, gp140 TV 1, gp41 HxBc2, gp70 V1 V2 CN54, gp70 V1 V2 Clade AE, m29091 peptide, p17 Clade C, and p24 HxBc2). These assays were transformed in the following manner prior to analysis: *transformed value = log10(original assay value +1)*

To reduce the dimensionality of the systems serology datasets before analysis, we identified the antigens for each of the above Fc-specificity assays that were most representative. This was done by determining which antigens for a given Fc-specificity assay yielded responses that were most strongly correlated to the 25% trimmed mean computed across all antigens for the same Fc-specificity assay. For all Fc-specificity assays except huFcgRIIIb, the responses for the different antigens were generally highly correlated. The antigen “gp120 TV 1” was identified as the most representative antigen overall for these assays as it ranked in the top 4 antigens for 8/10 assays and when it ranked lower the correlation to the trimmed mean was always > 0.85. For huFcgRIIIb, the responses exhibited greater antigen-dependence and the antigen “gp120 CM235” was the most representative antigen as it exhibited the strongest correlation to the overall trimmed mean. By identifying the representative antigens for the Fc specificity assays, we collapsed the 286 Fc specificity (11) X antigen (26) matrix into a matrix of 11 Fc specificity responses readouts.

After the above pre-filtering and transformations were completed, the final adaptive immune response/systems serology matrix consisted of 73 responses for the 52 animals (Supplemental Table – 17).

Integrating innate and adaptive immune responses

Given the diverse array of signaling pathways triggered by the panel of adjuvant formulations, we hypothesized that it would be possible to identify associations between vaccine triggered innate and adaptive immune responses that were specific to subsets of adjuvants and associations that were generally applicable across all adjuvants. To explore these possibilities, we performed analyses that consisted of discovering innate/adaptive associations using data from distinct sets of adjuvants, and by analyzing all adjuvants together. There were four adjuvant-specific subsets for the correlation analysis: (1) alum & alum/TLR4; (2) alum & alum/TLR7; (3) MF59 & ANE/TLR4; and (4) MF59 & ANE/TLR7. This analysis started from the list of modules up-regulated by all adjuvants (Supplemental Table 8) and correlated them to all of the adjuvant-responsive adaptive immune responses (Supplemental Table 17). A Spearman rank correlation analysis was performed which tested for the association between each module and each adaptive immune response. Innate/adaptive associations that were significantly correlated ($p<0.05$, FDR<0.2, two-sided test) when including the no-adjuvant group were identified and then tested again the no-adjuvant group was excluded. The surviving significant set of innate adaptive correlations were identified (Supplemental Table 21), and the representative genes from that exhibited the same correlation pattern as the parent modules were also identified (Supplemental Tables 22-23).

Correlations between the module/adaptive response profiles themselves (Supplemental Table 24) were also performed to explore similarities and differences between the adjuvant subsets (Supplemental Table 25). The distinct correlation patterns observed for different adjuvant subsets (Fig 5a, Suppl. Fig 7a) suggested that the means by which innate immunity imprints adaptive responses may exhibit a strong dependence on the context provided by the adjuvant platform employed. We thus compared the innate/adaptive correlation profiles for all innate and adaptive immune responses indicated in Figure 5a for all 5 adjuvant subsets (Suppl. Tables 24-25). While the overall correlation profile for the alum and alum/TLR7 subset was largely similar (Rho=0.64, $p=10^{-60}$), other correlation profiles were strongly anti-correlated (for example, alum and alum/TLR7 vs. alum and alum/TLR4; Rho=-0.52, $p=10^{-37}$) and others were not correlated at all (for example, all adjuvants vs. MF59 & ANE/TLR4). This result shows that for different adjuvant platforms, increasing a particular innate immune response may have opposing effects on the subsequent adaptive immune response.

Supplemental Tables

The following tables are in: Adjuvant Blood Supplementary Tables.xlsx

Table S1. (*SupTab01_MatrixLog2FoldChanges*): Normalized filtered log 2 gene expression fold-changes compared to pre-vaccination.

Table S2. (SupTab02_RNA.Sample.Table): RNA sample table – which NHP from which group have which time points.

Table S3. (SupTab03_TallyOfInnateResp.G): Tally of significantly regulated innate immune responses (genes) for each adjuvant.

Table S4. (SupTable04_InnateRespSumTab.G): Coded summary table for adjuvant-specific innate immune responses (genes).

Table S5. (SupTab05_ModuleDefinitions): Module definitions indicating which genes belong to which module at which time point.

Table S6. (SupTab06_ModuleData): Matrix of normalized pre-processed module response data that was used in the analyses.

Table S7. (SupTab07_TallyOfInnateResp.M): Tally of significantly regulated innate immune responses (modules) for each adjuvant.

Table S8. (SupTable08_InnateRespSumTab.M): Coded summary table for adjuvant-specific innate immune responses (Modules, up-regulated).

Table S9. (SupTab09_InnateResponseSimila.G): Fisher exact test results for evaluating associations between innate immune responses (genes) that are regulated by different adjuvants.

Table S10. (SupTab10_InnateResponseSimila.M): Fisher exact test results for evaluating associations between innate immune responses (modules) that are regulated by different adjuvants.

Table S11. (SupTab11_EffectOfTLR4.7onAlum.G): Effect of TLR4 or TLR7 ligand on Alum-induced genes

Table S12. (SupTab12_EffectOfTLR4.7onAlum.M): Effect of TLR4 or TLR7 ligand on Alum-induced modules

Table S13. (SupTab13_EffectOfTLR4.7onMF59.G): Effect of TLR4 or TLR7 ligand on MF59-induced genes

Table S14. (SupTab14_EffectOfTLR4.7onMF59.M): Effect of TLR4 or TLR7 ligand on MF59-induced modules

Table S15. (SupTab15_EffectOfAlum.MF59onT4): Effect of Alum or MF59 co-formulation on TLR4-induced genes

Table S16. (SupTab16_EffectOfAlum.MF59onT7): Effect of Alum or MF59 co-formulation on TLR7-induced genes

Table S17. (SupTab17_AdaptiveImmuneData): Matrix of normalized pre-processed adaptive immune response data that was used in the correlation analyses.

Table S18. (SupTab18_TallyOfRegulatedAdaptR): Tally of significantly regulated adaptive immune responses for each adjuvant.

Table S19. (SupTable19_AdaptiveRespSumTab): Coded summary table for adjuvant-specific adaptive immune responses.

Table S20. (SupTab20_AdaptiveResponseSimila): Fisher exact test results for evaluating associations between adaptive immune responses regulated by different adjuvants.

Table S21. (SupTab21_ModuleCorrWithAdapResp): Significant correlations between modules and specific adaptive immune responses for specific adjuvant subsets.

Table S22. (SupTab22_RepGenesFromModuleCorr): Representative genes from the modules significantly correlated to adaptive immune responses in Supplemental Table 21.

Table S23. (SupTab23_Gene.ModuleKeyforST22): Table indicating module memberships for genes in Supplemental Table 22.

Table S24. (SupTab24_ModuleVsAdaptiveCorrel): Spearman rho values for correlations between modules and adaptive immune responses for different adjuvant subsets, computed excluding the no adjuvant group.

Table S25. (SupTab25_CorOfCorForAdjSubsets): Spearman rank correlation statistics comparing adjuvant subsets in terms of Module-by-Adaptive response correlation coefficients (Supplemental Table 24).

Table S26. (SubTab26_SystemsSerologyData): Compiled results of the systems serology analysis, showing results for NK cell activation, ADCD, ADCC and ADCP.

Supplementary Figures

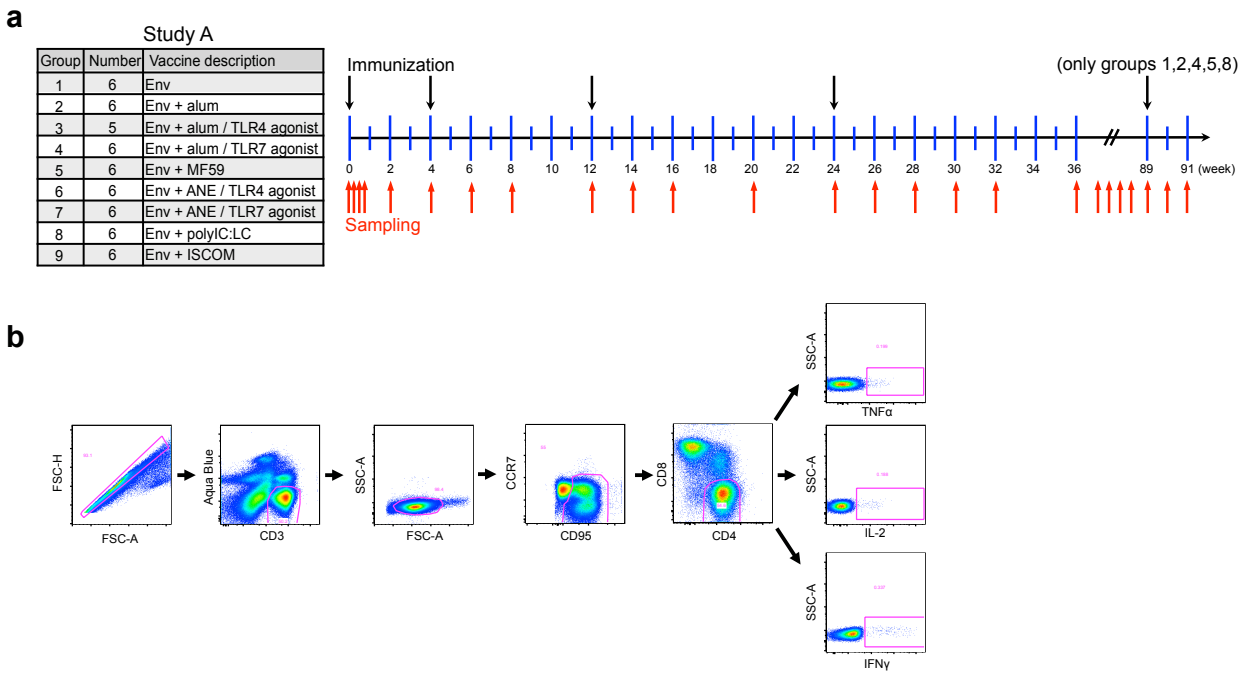

Figure S1. Study overview and flow cytometry gating. (**a**) The study was composed of 9 vaccine groups with vaccinations give in a homologous prime-boost fashion at 0, 4, 12 and 24 weeks (black arrows). Blood sampling was taken during the first hours and days after the prime, and then following at 2-4 week intervals (red arrows). ANE, adjuvant nano-emulsion; pIC:LC, polyinosinic-polycytidylic acid/ carboxymethylcellulose; ISCOM, immune stimulator complexes. (**b**) Flow cytometry gating used to measure T cell responses following intracellular cytokine staining in PBMCs. Cytokine positive cells are defined as CD95+/CD4+ and TNFα, IL-2, or IFNγ+.

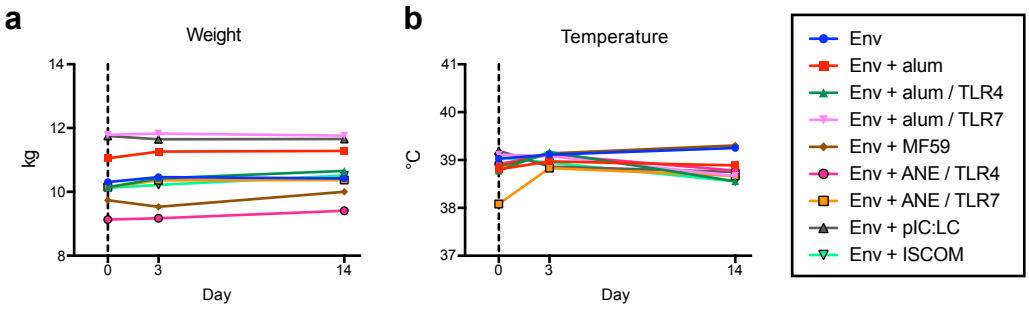

Figure S2. NHP physiological data. (**a**) Body weights and (**b**) temperature were measured following the first vaccination. Data points represent vaccine group medians; vertical dashed lines indicate immunization.

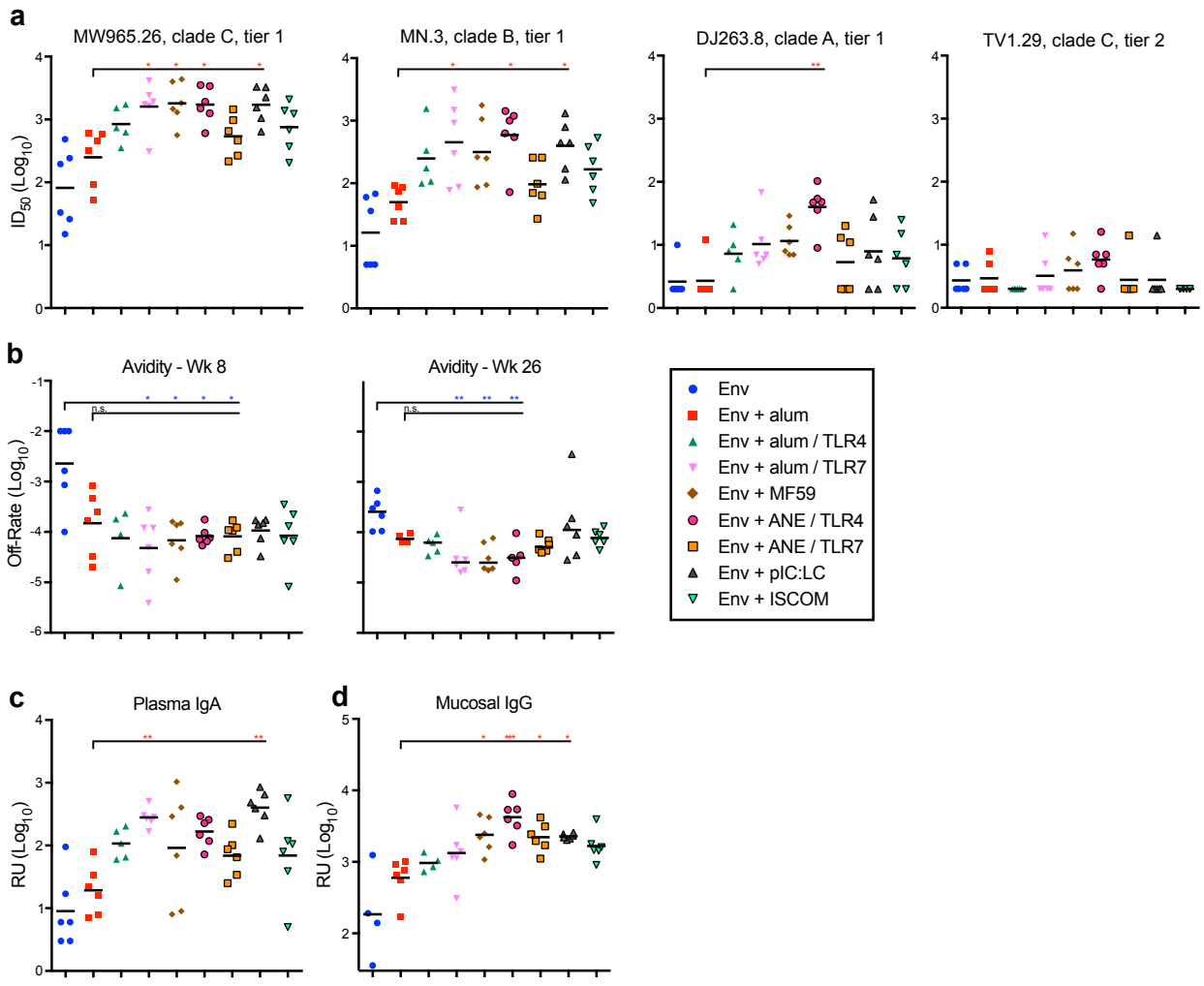

Figure S3. Expanded serological analysis at peak time points. (**a**) Plasma neutralization of clade A (DJ263.8), B (MN.3) and C (MW965.26 and TV1.29) Env-bearing pseudoviruses at week 26. (**b**) Serum avidity at week 8 and 26 for measured by SPR; off-rates are shown to control for differences in antibody concentration between groups. (**c**) IgA binding titers at week 26. (**d**) Mucosal IgG binding titers at week 30. TV1 gp140ΔV2 protein was used for mucosal IgG and avidity; horizontal bars indicate medians; RU, relative units; MFI, median fluorescent intensity; *, p<0.05; **, p<0.01; ***, p<0.001; n.s., by the Kruskal-Wallis test in which the Env alone or Env+alum group (as indicated) were set as the control.

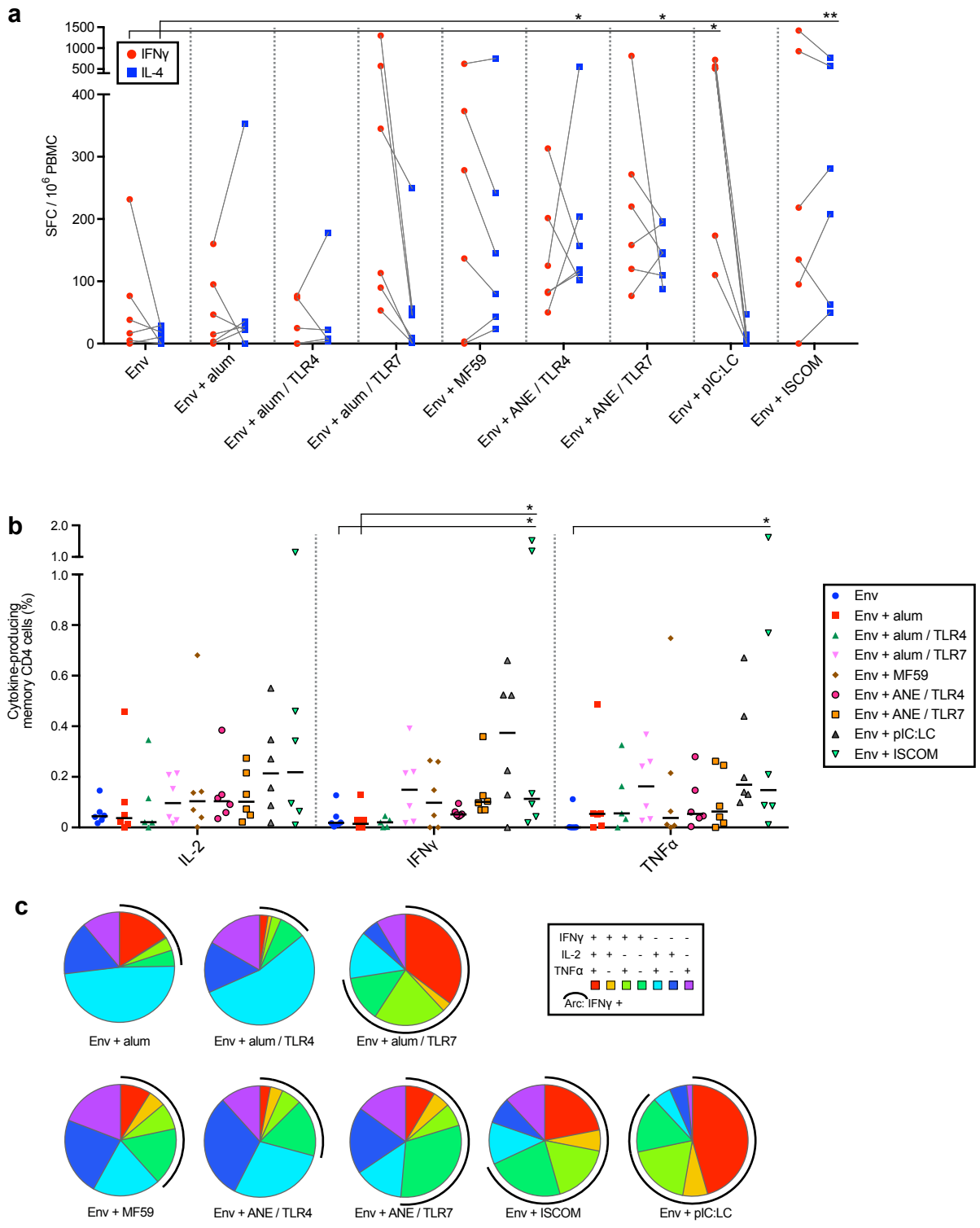

Figure S4. The effects of adjuvants on the magnitude and quality of Env-specific T cell responses. (**a**) Week 26 PBMCs were stimulated with clade C Env peptides and analyzed by ELISpot to detect the secretion of IFNγ or IL-4. Horizontal bars indicate group medians. (**b**) Week 26 PBMCs were stimulated with clade C Env peptides, stained for intracellular cytokines and analyzed by flow cytometry for the production of IL-2, IFNγ and TNFα. Horizontal bars indicate group medians. (**c**) Boolean gating was

employed to analyze the combination of cytokines on a per cell basis. Pie charts indicate the fraction of cells producing each possible combination of cytokines. For ICS, PBMC were stimulated with clade C Env peptides or media alone; data points indicate background-subtracted responses. Black arc indicates total $IFN\gamma^+$ fraction. Data are plotted as the median fraction per animal of total memory CD4 T cells expressing each cytokine. *, $p<0.05$; $p<0.05$; **, by the Kruskal-Wallis test in which the Env alone or Env+alum group (as indicated) were set as the control.

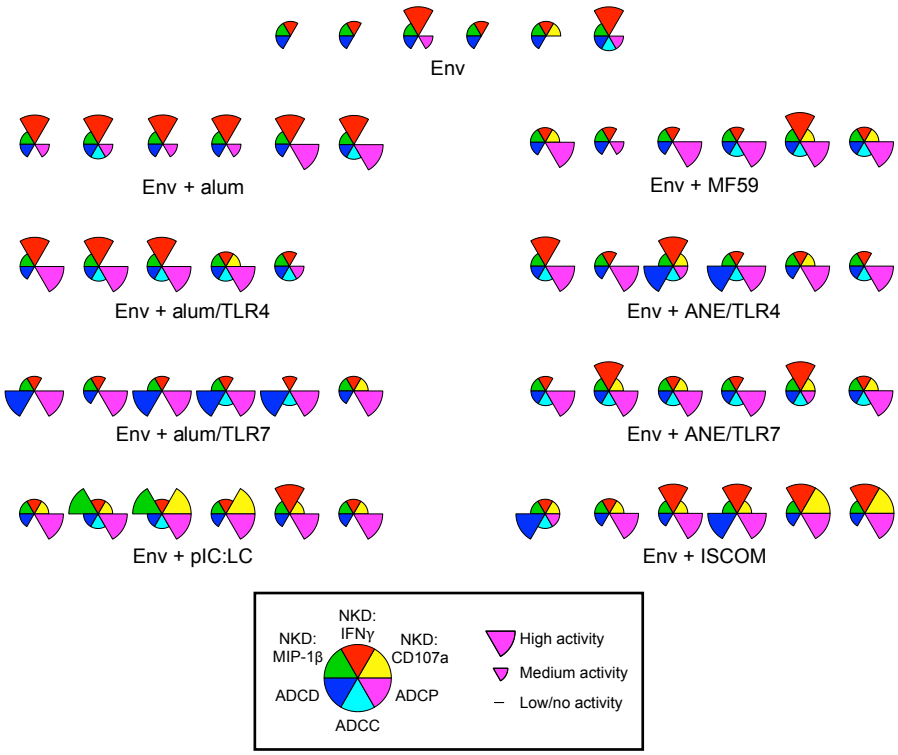

Figure S5. Pie charts depicting the relative NK cell cytokine and effector function response for each vaccine group. Each pie chart represents the response from an individual animal. NKD, natural killer cell degranulation; ADCD, antibody-dependent complement deposition; ADCC, antibody-dependent cellular cytotoxicity; ADCP, antibody-dependent cellular phagocytosis.

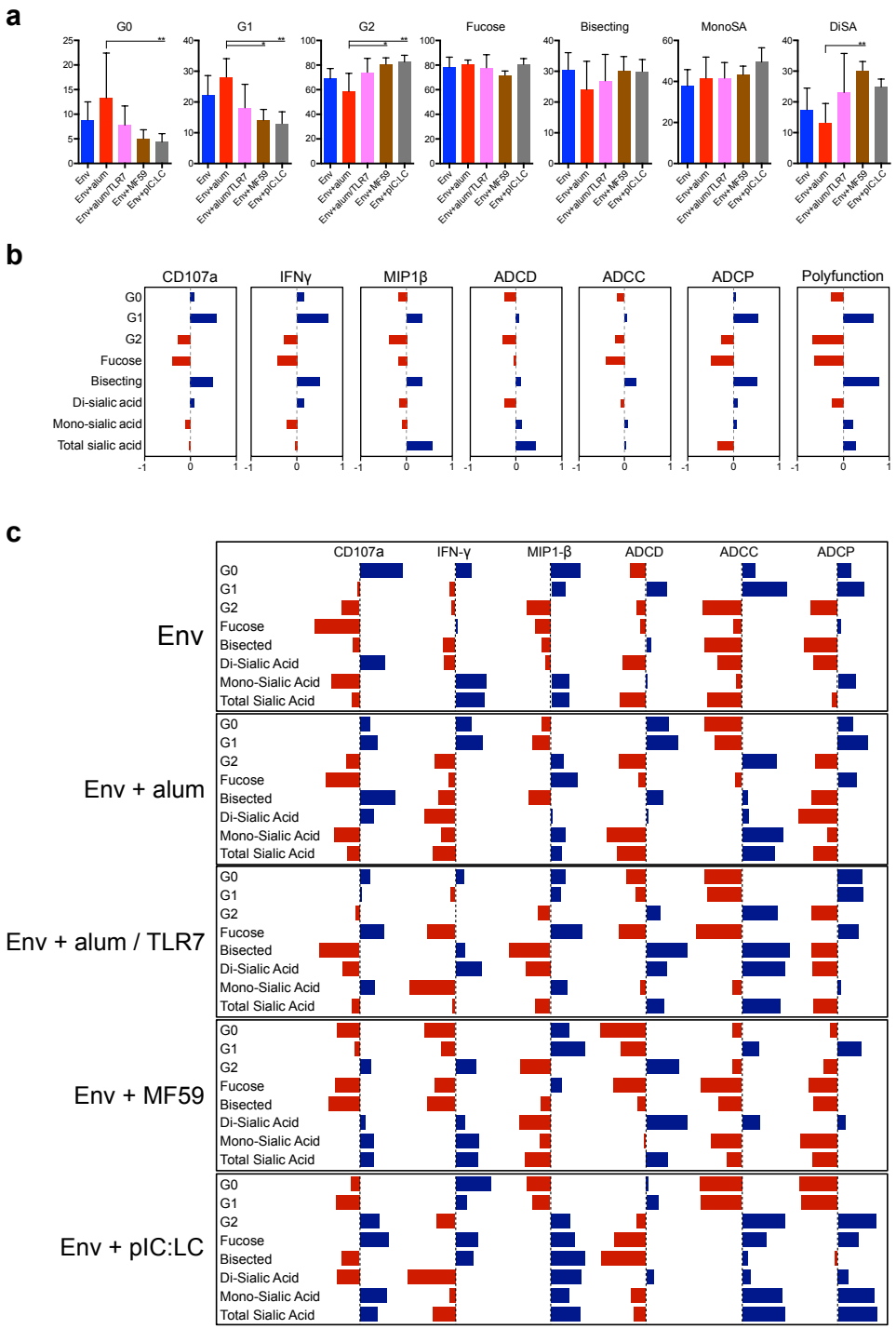

Figure S6. Systems serology analysis of IgG glycosylation and antibody effector functions. Serum was analyzed after the third immunization, at week 14. (**a**) Glycosylation structures present on antigen-specific Ig purified from sera. *, p<0.05; p<0.05; **, by the Kruskal-Wallis test in which the Env+alum group was set as the control. (**b**) Correlations of glycan structures for each antibody effector function. (**c**) Correlations between glycan structures and antibody effector functions parsed by vaccine group. Only a subset of vaccine groups is shown, for simplicity. ADCD, antibody-dependent complement deposition; ADCC, antibody-dependent cellular cytotoxicity; ADCP, antibody-dependent cellular phagocytosis. Blue bars= positive correlation; red bars= negative correlation.

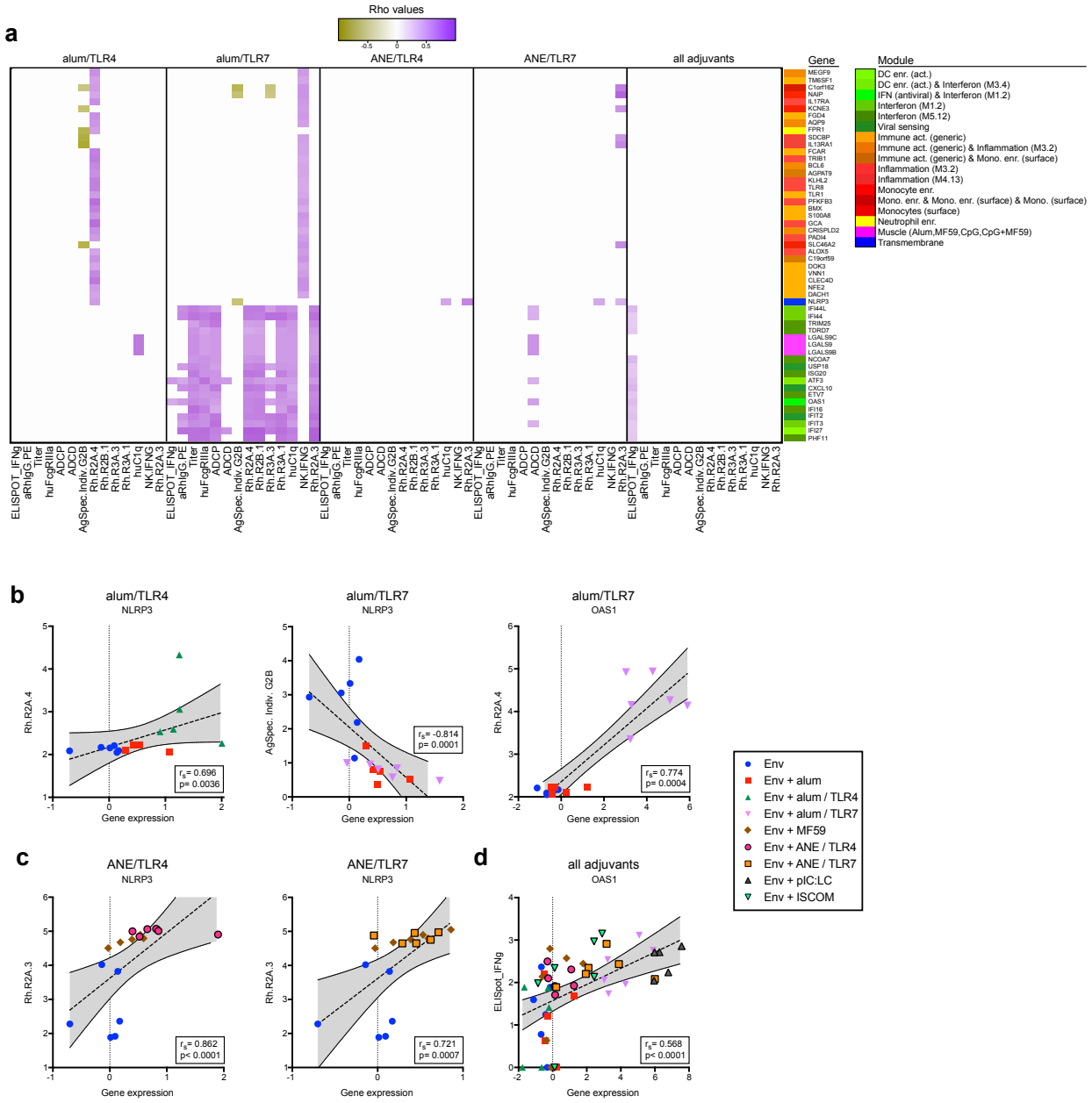

Figure S7. Correlations between individual innate genes and adaptive immune functional characteristics. (**a**) Expression data from innate genes were correlated with function characteristics including antibody titer and effector functions, F_C receptor binding, and T and NK cell cytokines. Gene module assignments are indicated by color code. The left 2 panels show correlations derived from the unadjuvanted group, with alum alone and alum/TLR4 or 7. The 3rd and 4th panels show correlations derived from the unadjuvanted group, with MF59 alone and ANE/TLR4 or 7. Correlations that were common to all adjuvant groups are shown in the far right panel. (**b**-**d**) Representative scatter plots show correlations for a group of vaccines between a representative gene (NLRP3 of the inflammasome, or OAS1 of the interferon response) and either antigen-specific individual G2B glycan, rhesus F_C receptor 2A.4 binding, or 2A.3 binding. (**b**) Alum-based formulations; (**c**) ANE-based formulations; (**d**) all adjuvant groups. For representative scatter plots, the correlation r_s and p-values are displayed numerically; dashed lines indicate linear regressions; grey shading highlights the 95% CI.

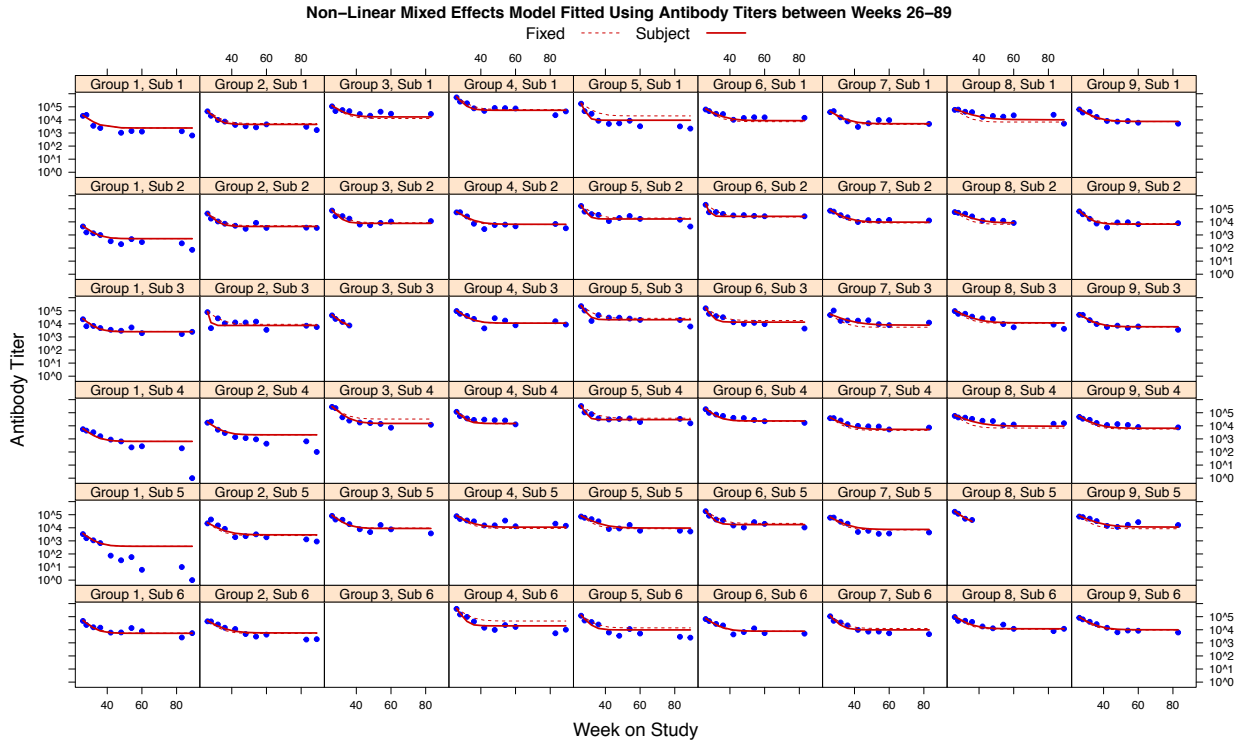

Figure S8. Fitted values from the non-linear mixed effects model employed to estimate antibody titer half-lives in Figure 1C. The model was fitted using antibody titers measured between weeks 26-89, i.e., after completing the primary immunization series. The fitting model is described above in the Supplementary Methods.

Supplementary References

1. Traquina P, Morandi M, Contorni M, Van Nest G. MF59 adjuvant enhances the antibody response to recombinant hepatitis B surface antigen vaccine in primates. *J Infect Dis*. 1996;174(6):1168-1175.
2. Li M, Gao F, Mascola JR, et al. Human immunodeficiency virus type 1 env clones from acute and early subtype B infections for standardized assessments of vaccine-elicited neutralizing antibodies. *J Virol*. 2005;79(16):10108-10125.
3. Seaman MS, Janes H, Hawkins N, et al. Tiered categorization of a diverse panel of HIV-1 Env pseudoviruses for assessment of neutralizing antibodies. *J Virol*. 2010;84(3):1439-1452.
4. Wu X, Zhou T, O'Dell S, Wyatt RT, Kwong PD, Mascola JR. Mechanism of human immunodeficiency virus type 1 resistance to monoclonal antibody B12 that effectively targets the site of CD4 attachment. *J Virol*. 2009;83(21):10892-10907.
5. Tomaras GD, Yates NL, Liu P, et al. Initial B-cell responses to transmitted human immunodeficiency virus type 1: virion-binding immunoglobulin M (IgM) and IgG antibodies followed by plasma anti-gp41 antibodies with ineffective control of initial viremia. *J Virol*. 2008;82(24):12449-12463.
6. Zolla-Pazner S, deCamp A, Gilbert PB, et al. Vaccine-induced IgG antibodies to V1V2 regions of multiple HIV-1 subtypes correlate with decreased risk of HIV-1 infection. *PLoS One*. 2014;9(2):e87572.
7. Yates NL, Liao HX, Fong Y, et al. Vaccine-induced Env V1-V2 IgG3 correlates with lower HIV-1 infection risk and declines soon after vaccination. *Sci Transl Med*. 2014;6(228):228ra239.
8. Haynes BF, Gilbert PB, McElrath MJ, et al. Immune-correlates analysis of an HIV-1 vaccine efficacy trial. *N Engl J Med*. 2012;366(14):1275-1286.
9. Flynn BJ, Kastenmuller K, Wille-Reece U, et al. Immunization with HIV Gag targeted to dendritic cells followed by recombinant New York vaccinia virus induces robust T-cell immunity in nonhuman primates. *Proc Natl Acad Sci U S A*. 2011;108(17):7131-7136.
10. Lynch HE, Stewart SM, Kepler TB, Sempowski GD, Alam SM. Surface plasmon resonance measurements of plasma antibody avidity during primary and secondary responses to anthrax protective antigen. *J Immunol Methods*. 2014;404:1-12.
11. Gentleman RC, Carey VJ, Bates DM, et al. Bioconductor: open software development for computational biology and bioinformatics. *Genome Biol*. 2004;5(10):R80.
12. Quinn KM, Zak DE, Costa A, et al. Antigen expression determines adenoviral vaccine potency independent of IFN and STING signaling. *J Clin Invest*. 2015;125(3):1129-1146.
13. Obermoser G, Presnell S, Domico K, et al. Systems scale interactive exploration reveals quantitative and qualitative differences in response to influenza and pneumococcal vaccines. *Immunity*. 2013;38(4):831-844.
14. Li S, Rouphael N, Duraisingham S, et al. Molecular signatures of antibody responses derived from a systems biology study of five human vaccines. *Nat Immunol*. 2014;15(2):195-204.
15. Mosca F, Tritto E, Muzzi A, et al. Molecular and cellular signatures of human vaccine adjuvants. *Proc Natl Acad Sci U S A*. 2008;105(30):10501-10506.
16. Mahan AE, Tedesco J, Dionne K, et al. A method for high-throughput, sensitive analysis of IgG Fc and Fab glycosylation by capillary electrophoresis. *J Immunol Methods*. 2015;417:34-44.
17. Ackerman ME, Moldt B, Wyatt RT, et al. A robust, high-throughput assay to determine the phagocytic activity of clinical antibody samples. *J Immunol Methods*. 2011;366(1-2):8-19.
18. Darrah PA, Patel DT, De Luca PM, et al. Multifunctional TH1 cells define a correlate of vaccine-mediated protection against Leishmania major. *Nature medicine*. 2007;13(7):843-850.
19. Gomez-Roman VR, Florese RH, Patterson LJ, et al. A simplified method for the rapid fluorometric assessment of antibody-dependent cell-mediated cytotoxicity. *J Immunol Methods*. 2006;308(1-2):53-67.
20. Chung AW, Ghebremichael M, Robinson H, et al. Polyfunctional Fc-effector profiles mediated by IgG subclass selection distinguish RV144 and VAX003 vaccines. *Sci Transl Med*. 2014;6(228):228ra238.